sciendo

Int. J. of Applied Mechanics and Engineering, 2020, vol.25, No.4, pp.175-190
DOI: 10.2478/ijame-2020-0057

TRANSIENT HEAT AND MASS TRANSFER OF HYDROMAGNETIC EFFECTS ON THE FLOW PAST A POROUS MEDIUM WITH MOVABLE VERTICAL PERMEABLESHEET

A.M. OKEDOYE
Department of Mathematics and Computer Science
Federal University of Petroleum Resources
Effurun, NIGERIA
E-mail: okedoye.akindele@fupre.edu.ng

S.O. SALAWU*
Department of Mathematics, Landmark University
Omu-aran, NIGERIA
E-mail: kunlesalawu2@gmail.com

An unsteady flow of heat and species transport through a porous medium in an infinite movable vertical permeable flat surface is considered. The hydromagnetic chemical reactive fluid flow is stimulated by the thermal and solutant convection, and propelled by the movement of the surface. The formulated nonlinear flow equations in time space are solved analytically by asymptotic expansions to obtain solutions for the flow momentum, energy and chemical concentration for various thermo-physical parameters. The existence of flow characteristic is defined with the assistance of the flow parameters. In the study, the impact of some pertinent flow terms is reported and discussed. The study revealed that the species boundary layer increases with a generative chemical reaction and decreases with a destructive chemical reaction. Also, arise in the generative species reaction term reduces the flow momentum for the cooling surface. The impact of other flow governing parameters is displayed graphically as well as the fluid wall friction, wall energy and species gradients. The results of this study are important in chemical thermal engineering for monitoring processes to avoid solution blow up.

Key words: movable plate, porosity, suction, perturbation method, MHD flow.

1. Introduction

The flow of convective solutant and thermal buoyancy fluid through a porous vertical surface is getting substantial responsiveness from several scientists because of its diverse usefulness in the area of geophysical and cosmical sciences. Absorbent surfaces are suitable in percolation processes, in keeping the temperature of a heated body constant and in maintaining effective heat lagging. The mass transfer phenomena are connected with the study of the solar surface and its stellar structure [1-7]. Its source is similar to heat difference instigated by the non-uniform temperature generation, which in various circum stances is attributed not only to convective currents formation but also to fierce ignitions. Fluid flow over an oscillating vertical surface has numerous technological and industrial applications. In a very essential sense, an oscillatory motion can be seen as an expression of a transient free surface fluid motion influenced by gravitational forces. That is, transient flow with free surface deformation can be seen as a type of oscillating flow, Salawu *et al*. [8, 9]. Considering composite forces in the fluids motion, the internal motions of the fluid particles and the geometry of the free surface show the effect of the interface between force of gravity and

*To whom correspondence should be addressed

pressure force. The amplitude of the flow characteristics does not reduce except the viscous forces that acted on it. Hence, it is essential to examine this phenomenon and its relation to an oscillatory hydromagnetic fluid over a moving vertical permeable sheet.

The Navier-Stokes equation was firstly solved analytically by Stokes [10], the equation has to do with the incompressible viscous fluid flow through an oscillatory horizontal wall. Turbatu *et al* [11] examined an incompressible viscous liquid flow past an oscillatory boundless wall with rising or reducing amplitude of the oscillation flow rate. Soundalgekar *et al.*[12] studied analytically the solution of a convective magnetohydromagnetic flow over a wavering wall. Okedoyeand Ayeni [13] examined the computational solution of energy and species transport in a hydromagnetic flow liquid in the presence of Arrhenius heat generation and species reaction in an elongated vertical porous channel. Das *et al*. [14] reported on the impact of energy and species transport of an incompressible conducting liquid flow in porous media with a permeable plate. They obtained the momentum, heat field and mass fields by the perturbation method. The Schmidt number and magnetic termdiscouraged the flow momentum distribution while the heat source, porosity, solutant, thermal Grashof terms had an increasing influence on the flow rate profile. Other relevant literature reports could be found in [15-19].

Currently, Rajput and Kumar [20] investigated a hydromagnetic flow with variable mass diffusion and temperature over a moving vertical sheet. They observed that the velocity increases when the mass Grashof number increases and decreases when the Hartmann number increases. The flow of an electrically conducting fluid with heat species transfer model for an incompressible free convective was presented by Moniem and Hassani [21]. They were able to establish that magnetic parameter, heavier diffusion species slow down the velocity while an inverse porosity term enhanced the velocity. Recently, Ahmed *et al.* [22] discussed transient MHD flow with the impact of first order species reaction and radiation for a viscous liquid past accelerating walls with adaptable heat. The Laplace transform method was adopted as the solution technique. Their investigation revealed that the fluid flow rate diminishes as the area adjacent to the wall and the rate of heat transfer reduce radiation absorption. While Chen *et al.* [23] studied the impact of a coupled electromagnetic flow in the fluid metal fusion manifold of a blanket. The work of [24, 25] discussed the unsteady flow of mass and thermal convection for a MHD fluid flow through saturated media embedded in an inclined accelerated exponentially permeable plate. They used the Laplace transform to obtain the solution. The result helps understand the dragging force effect on the cooled/heated inclined plates. In their study, Hemamalin and Kumar [26] analyzed the effect of the unsteady viscous liquid flow over a porous infinite uniformly moved vertical plates through porous media with adaptable heat using analytical methods. They observed that the flow momentum decreases with rising values of modified buoyance forces while the heat field rises with the enhancing time variation. The exact results for a single dimensional viscous fluid flow in an unsteady laminar MHD boundary layer flow past an unbounded exponentially moved wall in the existence of a perpendicular magnetic field was obtained by [27-30]. The analytical results for the non-dimensional boundary layer are obtained by the Laplace transform method. It was observed that the flow rate is encouraged with rising porosity and Grashof number terms, and diminishes with enhancing values of radiation and magnetic terms.

The present study examines the flow of chemical diffusion in a porous medium with thermal and species convection in a vertical medium. The transient thermal chemical reactive flow solution with boundary layers over an infinite vertical moving permeable surface is analytically provided. With chemical species, heat absorption and suction, the surface moves in its own plane. The parameter dependent solutions are obtained using perturbation techniques. The results are graphically demonstrated for the embedded terms and quantitatively discussed with physical implication. The study will contribute to the thermal science, chemical engineering and technology and help understand the safe and unsafe conditions of thermal molecular reactive diffusion in order to avoid solution blow-up.

2. Formulation of the problem

The buoyancy gravity forces along with the Navier–Stokes equation describe the flow fluid motion under consideration. The gravity is affected by the inviscid flow equation and this can be represented in the

wave equation form. Consider an incompressible, unsteady conducting liquid flow over a moving permeable flat wall (Fig.1). The *x*-axis is taken along the upward vertical direction of the flat sheet and it is assumed that the *y* - axis is normal to the upward direction of the wall. Suppose correspondingly, *u* and *v* are the flow momentum modules in the direction of the *x*- and *y* - axes. Taken that the flat surface is in motion with velocity $u = v_0$ in its own plane at time *t=0*, and at time $t > 0$, the velocity grows to a finite velocity $u = v_w$.

In vector form, the governing continuity, momentum, energy and species equations are respectively expressed as

$$\nabla \cdot V = 0, \tag{2.1}$$

$$\rho(V \cdot \nabla)V = -\nabla p + \mu \nabla^2 V + \rho(J \times B) - \frac{\mu}{K} V, \tag{2.2}$$

$$\rho Cp(V \cdot \nabla)T = k\nabla^2 T - \nabla \cdot q + Q, \tag{2.3}$$

$$(V \cdot \nabla)C = D\nabla^2 C - R \tag{2.4}$$

where V is the fluid velocity vector, K is the Darcy porous term, q denotes the thermal radiation, Q is the heat source or sink, R represents the chemical reaction and J is the current density which can be defined as $J = \sigma(E + V \times B - J \times B)$ and $B = (0, B(x))$. Here, E is the electric field and σ denotes the electric conductivity.

Applying Darcy's law for porosity, the unsteady equations for the flow rate, energy and concentration balance in a boundary layer flow are described as

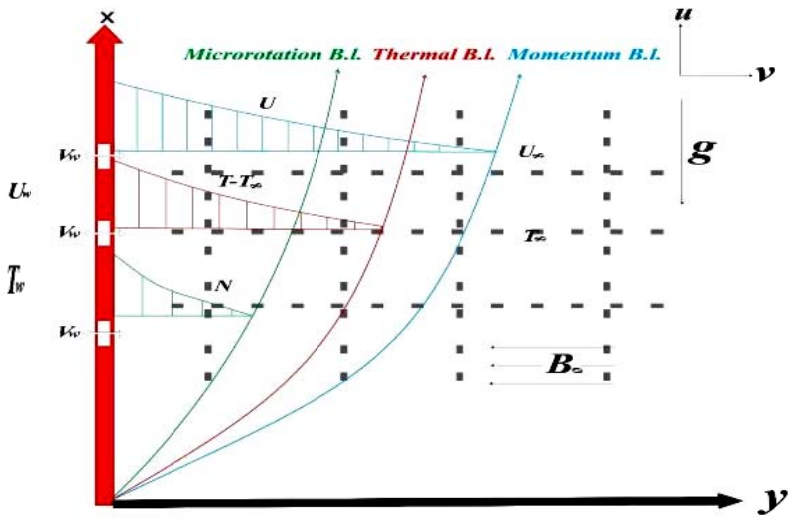

Fig.1.The flow schematic geometry.

$$\frac{\partial v}{\partial y} = 0, \tag{2.5}$$

$$\frac{\partial u}{\partial t} + v\frac{\partial u}{\partial y} = \upsilon \frac{\partial^2 u}{\partial y^2} - \frac{\sigma B_0^2}{\rho} u + \frac{\beta_\tau g}{\rho}(T - T_\infty) + \frac{\beta_c g}{\rho}(C - C_\infty) - \frac{v}{A} u, \tag{2.6}$$

$$\frac{\partial T}{\partial t}+v\frac{\partial T}{\partial y}=\frac{k}{\rho c_p}\frac{\partial^2 T}{\partial y^2}+\frac{Q}{\rho c_p}\left(T-T_\infty\right), \tag{2.7}$$

$$\frac{\partial C}{\partial t}+v\frac{\partial C}{\partial y}=D\frac{\partial^2 C}{\partial y^2}-R\left(C-C_\infty\right). \tag{2.8}$$

On ignoring the dissipation Joule heat, the boundary conditions take the form

$$u=0,\quad T=T_\infty,\quad C=C_\infty \quad \text{for all} \quad y,\quad t\le 0,$$

$$u=v_0,\quad v=-v_w,\quad T=T_w+\varepsilon e^{i\omega t},\quad C=C_w+\varepsilon e^{i\omega t},\quad y=0,\quad t>0, \tag{2.9}$$

$$u=0,\quad T=T_\infty,\quad C=C_\infty \quad \text{as} \quad y\to\infty,\quad t>0.$$

From Eq.(2.5) to Eqs (2.9), $v\left(y,t\right)=-v_0\left(1+\epsilon e^{i\omega t}\right)$ is defined for simplification of the equations. Applying the subsequent variables

$$u'=\frac{u}{\nu_w},\quad t'=\frac{tv_w^2}{4v},\quad y'=\frac{yv_w}{v},\quad A'=\frac{v_0^2}{v^2},\quad Q'=\frac{4Q\upsilon}{v_0^2},$$

$$\omega'=\frac{4\omega v}{v_0^2},\quad \varphi=\frac{C-C_\infty}{C_w-C_\infty},\quad \theta=\frac{T-T_\infty}{T_w-T_\infty}, \tag{2.10}$$

where the physical quantities maintain their respective meaning.

With the aid of Eq.(2.10) and on dropping primes $(')$, the equations governing the flow Eqs (2.6) – (2.9) together with the boundary conditions become

$$\frac{1}{4}\frac{\partial u}{\partial t}-\left(1+\varepsilon e^{i\omega t}\right)\frac{\partial u}{\partial y}=\frac{\partial^2 u}{\partial y^2}+\mathrm{Gr}(\theta+N\varphi)-\left(k_p+M\right)u, \tag{2.11}$$

$$\frac{\mathrm{Pr}}{4}\frac{\partial\theta}{\partial t}-\mathrm{Pr}\left(1+\varepsilon e^{i\omega t}\right)\frac{\partial\theta}{\partial y}=\frac{\partial^2\theta}{\partial y^2}+\mathrm{Pr}\beta\theta, \tag{2.12}$$

$$\frac{\mathrm{Sc}}{4}\frac{\partial\varphi}{\partial t}-\mathrm{Sc}\left(1+\varepsilon e^{i\omega t}\right)\frac{\partial\varphi}{\partial y}=\frac{\partial^2\varphi}{\partial y^2}-\alpha\mathrm{Sc}\varphi, \tag{2.13}$$

$$u=v_0(1+\varepsilon),\quad \theta=1,\quad \varphi=1,\quad \text{for all}\quad y,\quad t\le 0,$$

$$u=1,\quad \theta=1+\varepsilon e^{i\omega t},\quad \varphi=1+\varepsilon e^{i\omega t},\quad y=0,\quad t>0, \tag{2.14}$$

$$u\to 0,\quad \theta\to 0,\quad \varphi\to 0,\quad \text{as}\quad y\to\infty,\quad t>0$$

where all the emerging terms are described as follows

$$N=\frac{\beta_\tau\left(T_w-T_\infty\right)v}{\beta_c\left(C_w-C_\infty\right)},\qquad \mathrm{Gr}=\frac{g\beta_c\left(C_w-C_\infty\right)v}{\rho v_w^3 u_w},\qquad M=\frac{\sigma B_0^2 v}{\rho v_0^2},$$

$$\alpha=\frac{v_0^2 A}{v^2},\qquad \mathrm{Pr}=\frac{\mu c_p}{k},\qquad \beta=\frac{Q\upsilon}{v_w^2\rho c_p},\qquad \mathrm{Sc}=\frac{v}{D},\qquad \alpha=\frac{R\upsilon}{v_w^2}. \tag{2.15}$$

3. Method of solution

Unfortunately, it is challenging or not possible to get a general solution for the problem. To obtain solution to the dimensionless Eqs (2.11) – (2.13), a perturbation method in series expansion is adopted with the limit ε for the reliant variables. It is necessary because ε is small; thus we write according to Okedoye and Salawu [31]

$$\begin{aligned}
u(y,t)&=u_0(y)+\varepsilon e^{i\omega t}u_1(y)+O(\varepsilon^2)+\ldots.,\\
\theta(y,t)&=\theta_0(y)+\varepsilon e^{i\omega t}\theta_1(y)+O(\varepsilon^2)+\ldots.,\\
\mathrm{H}(y,t)&=\mathrm{H}_0(y)+\varepsilon e^{i\omega t}\mathrm{H}_1(y)+Oo(\varepsilon^2)+\ldots.
\end{aligned} \tag{3.1}$$

Using Eqs (3.1) in Eqs (2.11), (2.12) and (2.13) and then equating the harmonic and non-harmonic terms, and ignoring the terms with the coefficient of $\varepsilon \geq 2$, the mean motion state and the unsteady flow state of the governing equations are obtained as

$$\frac{d^2\theta_0}{dy^2}+\mathrm{Pr}\frac{d\theta_0}{dy}-\mathrm{Pr}\beta\theta=0,$$

$$\theta_0(0)=1,\qquad \theta_0(y)\to 0\quad \text{as}\quad y\to\infty, \tag{3.2}$$

$$\frac{d^2\varphi_0}{dy^2}+\mathrm{Sc}\frac{d\varphi_0}{dy}-\mathrm{Sc}\alpha\varphi_0=0,$$

$$\varphi_0(y)=1\quad \text{at}\quad y=0\quad \varphi_0(y)\to 0\quad \text{as}\quad y\to\infty, \tag{3.3}$$

$$\frac{d^2u_0}{dy^2}+\frac{du_0}{dy}-\left(M^2+k_p\right)u_0=-\mathrm{Gr}(N\theta_0-\varphi_0),$$

$$u_0(y)=0\quad \text{at}\quad y=0,\qquad u_0(y)\to 0\quad \text{as}\quad y\to\infty, \tag{3.4}$$

and

$$\frac{d^2\theta_1}{dy^2}+\Pr\frac{d\theta_1}{dy}-\Pr\left(\frac{i\omega}{4}-\beta\right)\theta_1=0,$$

$$\theta_1(y)=e^{i\omega t} \quad \text{at} \quad y=0, \quad \theta_1(y)\to 0 \quad \text{as} \quad y\to\infty, \tag{3.5}$$

$$\frac{d^2\varphi_1}{dy^2}+\mathrm{Sc}\frac{d\varphi_1}{dy}=\mathrm{Sc}\left(\frac{i\omega}{4}+\alpha\right)\varphi_1+\mathrm{Sc}\varphi_0,$$

$$\varphi_1(y)=1 \quad \text{at} \quad y=0, \quad \varphi_1(y)\to 0 \quad \text{as} \quad y\to\infty, \tag{3.6}$$

$$\frac{d^2u_1}{dy^2}+\frac{du_1}{dy}-\left(M^2+k_p+\frac{i\omega}{4}\right)u_1=k_pu_0-u'_0-\mathrm{Gr}(N\theta_1-\varphi_1),$$

$$u_1(y)=0 \quad \text{at} \quad y=0, \quad u_1(y)\to 0 \quad \text{as} \quad y\to\infty. \tag{3.7}$$

These equations are then analytically solved to get the momentum, concentration and heat field solution. Hence, Eqs (3.2) – (3.7) have the following solutions

$$\varphi_0(y)=e^{-my}, \quad \theta_0(y)=e^{-ny}, \quad u_0(y)=a_0e^{-ry}+a_1e^{-ny}+a_2e^{-my},$$

$$\varphi_1(y)=a_4e^{-\lambda y}+a_3e^{-my}, \quad \theta_1(y)=a_6e^{-sy}+a_5e^{-ny}, \tag{3.8}$$

$$u_1(y)=a_7e^{-\mu_1 y}+a_8e^{-ry}+a_9e^{-ny}+a_{10}e^{-my}+a_{11}e^{-sy}+a_{12}e^{-\lambda y}$$

where

$$n=\frac{1}{2}\left(\Pr+\sqrt{\mathbf{Pr}^2-4\Pr\beta}\right), \; s=\frac{1}{2}\left(\Pr+\sqrt{\Pr^2-4\Pr\left(\beta-\frac{i\omega}{4}\right)}\right),$$

$$m=\frac{1}{2}\left(\mathrm{Sc}+\sqrt{\mathrm{Sc}^2+4\mathrm{Sc}\alpha}\right), \; \lambda=\frac{1}{2}\left(\mathrm{Sc}+\sqrt{\mathrm{Sc}^2+4\mathrm{Sc}\left(\alpha+\frac{i\omega}{4}\right)}\right),$$

$$r=\frac{1}{2}\left(1+\sqrt{1+4\left(M+k_p\right)}\right), \; \mu=\frac{1}{2}\left(1+\sqrt{1+4\left(M+k_p+\frac{i\omega}{4}\right)}\right),$$

with

$$a_0=v_0-a_1-a_2, \quad a_1=\frac{-N\mathrm{Gr}}{n^2-n-\left(M+k_p\right)}, \quad a_2=\frac{\mathrm{Gr}}{m^2-m-\left(M+k_p\right)},$$

$$a_3=\frac{m\mathrm{Sc}}{m^2-m\mathrm{Sc}-\mathrm{Sc}\left(\alpha+\frac{i\omega}{4}\right)}, \quad a_4=1-a_3, \quad a_5=\frac{n\Pr}{n^2-n\Pr-\Pr\left(\beta-\frac{i\omega}{4}\right)}, \quad a_6=1-a_5,$$

$$a_7 = V_0 - \left(a_8 + a_9 + a_{10} + a_{11} + a_{12}\right), \qquad a_8 = \frac{a_0(k_p + r)}{r^2 - r - \left(M + k_p + \frac{i\omega}{4}\right)},$$

$$a_9 = \frac{a_1(k_p + n) - a_5 N\mathrm{Gr}}{r^2 - r - \left(M + k_p + \frac{i\omega}{4}\right)}, \qquad a_{10} = \frac{a_2(k_p + m) - a_3\mathrm{Gr}}{m^2 - m - \left(M + k_p + \frac{i\omega}{4}\right)},$$

$$a_{11} = \frac{-a_6 N\mathrm{Gr}}{s^2 - s - \left(M + k_p + \frac{i\omega}{4}\right)}, \qquad a_{12} = \frac{-a_4\mathrm{Gr}}{\lambda^2 - \lambda - \left(M + k_p + \frac{i\omega}{4}\right)}.$$

In Eq.(3.8), the functions $u_0(y)$, $\theta_0(y)$ and $\varphi_0(y)$ are respectively the mean flow rate, energy and mass distributions; and $u_1(y)$, $\theta_1(y)$ and $\varphi_1(y)$ denote the oscillatory momentum, heat and species fields. On using Eq.(3.8) in Eq.(3.1), the expected equations for the flow rate, heat and concentration are

$$\begin{aligned} u(y,t) &= a_0 e^{-ry} + a_1 e^{-ny} + a_2 e^{-my} + \\ &+ \varepsilon e^{i\omega}\left(a_7 e^{-\mu_1 y} + a_8 e^{-ry} + a_9 e^{-ny} + a_{10} e^{-my} + a_{11} e^{-sy} + a_{12} e^{-\lambda y}\right), \end{aligned} \tag{3.9}$$

$$\theta(y,t) = e^{-ny} + \varepsilon e^{2i\omega t}\left(a_6 e^{-sy} + a_5 e^{-ny}\right), \tag{3.10}$$

$$\varphi(y,t) = e^{-my} + \varepsilon e^{2i\omega t}\left(a_4 e^{-\lambda y} + a_3 e^{-my}\right). \tag{3.11}$$

Having obtained expressions for velocity, temperature and concentration, we then use a computer software package (Maple) to build up the imaginary and real parts, but the real part (our interest) of concentration, temperature and velocity are given as follows

$$\Re(\phi) = e^{-my} + \varepsilon\left(f_1\cos(\omega t) - f_2\sin(\omega t)\right) \quad \text{or} \quad \Re(\phi) = e^{-my} + \varepsilon\,|f_{12}|\cos(\omega t + \alpha_1),$$

$$\Re(\theta) = e^{-ny} + \varepsilon\left(g_1\cos(\omega t) - g_2\sin(\omega t)\right) \quad \text{or} \quad \Re(\theta) = e^{-ny} + \varepsilon\,|g_{12}|\cos(\omega t + \alpha_2),$$

$$\Re(u) = a_0 e^{-ry} + a_1 e^{-ny} + a_2 e^{-my} + \varepsilon\left(h_1\cos(\omega t) - h_2\sin(\omega t)\right)$$

or

$$\Re(u) = a_0 e^{-ry} + a_1 e^{-ny} + a_2 e^{-my} + \varepsilon|h_{12}|\cos(\omega t + \alpha_3)$$

where the fluctuating parts are given by the expressions

$$f_1 = b_1 e^{-my} + e^{-y\lambda_1}\left(b_3\cos(y\lambda_2) - b_2\sin(y\lambda_2)\right),$$

$$f_2 = b_2 e^{-my} - e^{-y\lambda_1}\left(b_2\cos(y\lambda_2) + b_3\sin(y\lambda_2)\right),$$

$$g_1 = b_4 e^{-ny} + e^{-ys_1}\left(b_6\cos(ys_2) - b_5\sin(ys_2)\right),$$

$$g_2 = b_5 e^{-ny} - e^{-ys_1}\left(b_5\cos(ys_2) - b_6\sin(ys_2)\right),$$

$$h_1 = b_7 e^{-ry} + b_9 e^{-ny} + b_{11} e^{-my} + e^{-ys_1}\left(b_{13}\cos(ys_2) - b_{14}(ys_2)\right) +$$
$$+ e^{-y\lambda_1}\left(b_{15}\cos(y\lambda_2) - b_{16}\sin(y\lambda_2)\right) + e^{-y\mu_1}\left(b_{17}\cos(y\mu_2) - b_{18}\sin(y\mu_2)\right),$$

$$h_2 = b_8 e^{-ry} + b_{10} e^{-ny} + b_{12} e^{-my} - e^{-ys_1}\left(b_{14}\cos(ys_2) + b_{13}(ys_2)\right) +$$
$$- e^{-y\lambda_1}\left(b_{16}\cos(y\lambda_2) + b_{15}\sin(y\lambda_2)\right) - e^{-y\mu_1}\left(b_{18}\cos(y\mu_2) - b_{17}\sin(y\mu_2)\right).$$

The amplitude $|f_{12}| = \sqrt{f_1^2 + f_2^2}$, $|g_{12}| = \sqrt{g_1^2 + g_2^2}$, $|h_{12}| = \sqrt{h_1^2 + h_2^2}$ and phase of concentration, temperature and velocity respectively are

$$\tan\Omega_1 = \frac{f_1}{f_2}, \quad \tan\Omega_2 = \frac{g_1}{g_2} \quad \text{and} \quad \tan\Omega_3 = \frac{h_1}{h_2}.$$

Skin-Friction: From the momentum field, the skin-friction is studied which is given as

$$c_f = \frac{T_f}{\rho u_\omega v_\omega} = \frac{d^2}{dy^2}u(y,t)\bigg|_{y=0}, \qquad \tau_f = \mu\frac{du}{dy}\bigg|_{y=0}.$$

The equation is transformed using the dimensionless quantities in Eq.(2.10) to have

$$c_f = \left(\frac{\partial u}{\partial y}\right)_{y=0}.$$

Then

$$c_f = -a_0 r - a_2 m - a_1 n + \varepsilon e^{2i\omega t}\left(-a_7\mu_1 - a_8 r - a_9 n + a_{10} m + a_{11} s + a_{12}\lambda\right), \tag{3.12}$$

$$\tau = -a_2 m - a_1 n - a_0 r + \epsilon\left(\tau_1\cos(\omega t) - \tau_1\sin(\omega t)\right)$$

or

$$\tau = -a_2 m - a_1 n - a_0 r + \epsilon|\tau_{12}|\cos(\omega t + \alpha_6)$$

where

$$\tau_1 = -rb_7 - nb_9 - mb_{11} - b_{13}s_1 - b_{14}s_2 - b_{15}\lambda_1 - b_{16}\lambda_2 - b_{17_{\mu_1}} - b_{18}\mu_2,$$

$$\tau_2 = b_{13}s_2 + b_{16}\lambda_1 - b_{17}\mu_2 - rb_8 - nb_{10} + b_{14}s_1 - b_{15}\lambda_2 + b_{18}\mu_1 - mb_{12}.$$

The skin friction amplitude is $\tau_{12} = \sqrt{\left(\tau_1^2 + \tau_2^2\right)}$ and the phase is given by $\tan\alpha_6 = \frac{\tau_2}{\tau_1}$.

Nusselt number: From Fourier's law, the heat gradient at the wall is obtained with the aid of the dimensionless variables of Eq.(2.10) as follows

$$\mathrm{Nu}=\frac{q_\omega v}{(T_\omega-T_\infty)Kv_\omega}=\frac{-d}{dy}\theta(yt)\Big|_{y=0}, \qquad q_\omega=-K\frac{dT}{dy}\Big|_{y=0}.$$

Hence,

$$\mathrm{Nu}=-n-\epsilon e^{2i\omega t}\left(sa_6+na_5\right), \tag{3.13}$$

$$\mathrm{Nu}=-n+\epsilon\left(\mathrm{Nu}_1\cos(\omega t)-\mathrm{Nu}_2\sin(\omega t)\right) \quad \text{or} \quad \mathrm{Nu}=-n+\epsilon\left|\mathrm{Nu}_{12}\right|\cos(\omega t+\alpha_5)$$

where

$$\mathrm{Nu}_1=-nb_4-b_5s_2-b_6s_1 \quad \text{and} \quad \mathrm{Nu}_2=-nb_5s_1-b_6s_2.$$

The amplitude is $\mathrm{Nu}_{12}=\sqrt{\left(\mathrm{Nu}_1^2+\mathrm{Nu}_2^2\right)}$ and phase of the Nusselt number $\tan\alpha_5=\dfrac{\mathrm{Nu}_2}{\mathrm{Nu}_1}$.

Sherwood number: The ratio of the scale length to the diffusive boundary layer viscosity is called the wall mass transfer known as the Sherwood number which is defined as

$$\mathrm{Sh}=\frac{J_\omega\, v}{(c_\omega-c_\infty)Dv_\omega}=-\frac{d}{dy}\varphi(y,t)\Big|_{y=0}, \qquad J_\omega=-D\frac{d\varphi}{dy}\Big|_{y=0} \text{ which implies}$$

$$\mathrm{Sh}=-m-\epsilon e^{2i\omega t}\left(\lambda a_4+ma_3\right), \tag{3.14}$$

$$\mathrm{Sh}=-m+\epsilon\left(\mathrm{Sh}_1\cos(\omega t)-\mathrm{Sh}_2\sin(\omega t)\right) \quad \text{or} \quad \mathrm{Sh}=-m+\epsilon\mathrm{Sh}_{12}\cos(\omega t+\alpha_4)$$

where

$$\mathrm{Sh}_1=-mb_1-b_2\lambda_2-b_3\lambda_1 \quad \text{and} \quad \mathrm{Sh}_2=-mb_2+b_2\lambda_1-b_3\lambda_2.$$

The amplitude of Sh is $\left|\mathrm{Sh}_{12}\right|=\sqrt{\left(\mathrm{Sh}_1^2+\mathrm{Sh}_2^2\right)}$ and the phase $\tan\alpha_4=\dfrac{\mathrm{Sh}_2}{\mathrm{Sh}_1}$.

4. Discussion of results

The flow of transient energy and concentration transport over a boundless moving vertical permeable flat sheet with chemical reaction, heat absorption/generation and suction has been formulated and solved analytically by asymptotic expansions. To get the influence of some entrenched terms on the reactive fluid flow, the subsequent description is considered. The default Prandtl number values is taken as Pr = *0.71* (plasma). The default Schmidt number value is picked as (*0.60*) to denote the water vapour. All emerging terms are mainly selected as follows: $\mathrm{Gr}=0.4$, $N=0.3$, $M=0.5$, $k_p=0.2$, $\alpha=0.5$, $\beta=0.15$, $V_0=0.5$, $\epsilon=0.2$, ω and t were carefully chosen so that $\omega t=\pi/2$ except otherwise stated in each graph. The influence of each term on the mass, energy and flow rate distributions is displayed graphically. It should be noted that $\mathrm{Gr}>0$ and $\mathrm{Gr}<0$ depict the cooling and heating surface, respectively. Also, $\alpha<0$ and $\alpha>0$ represent generative and destructive chemical reactions, respectively. While $\beta<0$ and $\beta>0$ indicate heat generation and heat absorption, respectively.

4.1. Concentration distribution

The flow concentration field with the existence of external species, like water vapour, is illustrated in Figs 1–3. The flow is influenced by two terms, that is the chemical reaction term (α) and Schmidt number (Sc). In the analysis, the Schmidt number is chosen as *0.60*, thus the only parameter that affects the concentration distribution is α . The mass distribution is largely impacted by the external species. A study of Fig.1 shows that the mass distribution diminishes quicker than the reaction parameter (α) increases. The concentration boundary layer increases with increasing values of the chemical generative and decreases with rising chemical destructive term. Thus, a high chemical reaction parameter (destructive reaction) indicates a quicker decline in the flow mass. Figures 2 and 3 depict the behaviour of the fluid amplitude $|f_{12}|$ and phase $\tan\Omega_1$ of concentration profiles by varying the chemical reaction parameter. The flow concentration enhances with a rise in the chemical generative term $(\alpha < 0)$ and diminishes for the chemical destructive term $(\alpha > 0)$. Additionally, the phase of concentration oscillates repeatedly during which the effect reverses. This physically holds because when α is positively large, more chemical species are consumed.

4.2. Temperature field

The influence of β on the flow heat distribution is depicted in Figs 4-6. Figures 4 and 5 show that an increase in the absorption heat leads to rises in the flow bulk heat profile and the temperature amplitude while an increase in the heat generation lowers the bulk temperature field. Therefore, plate cooling occurs quicker as the heat generation term rises. Hence, it can be established that heat generation causes faster plate cooling. The temperature boundary layer declines as the flowing fluid moves far from the surface, its asymptotically approaches zero as it moves further from the sheet, and the heat increases due to an increase in the heat absorption. Thus the higher boundary layer occurs when heat generated

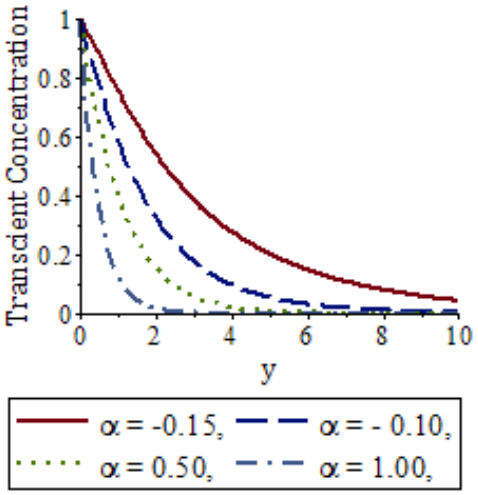

Fig.1. Variation of transient concentration for various values of α .

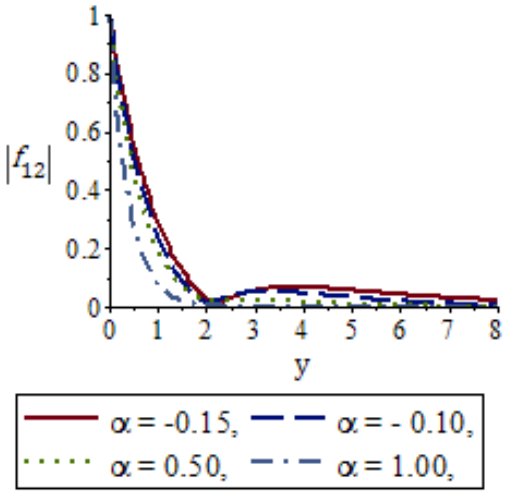

Fig.2. Amplitude of concentration profiles $(|f_{12}|)$.

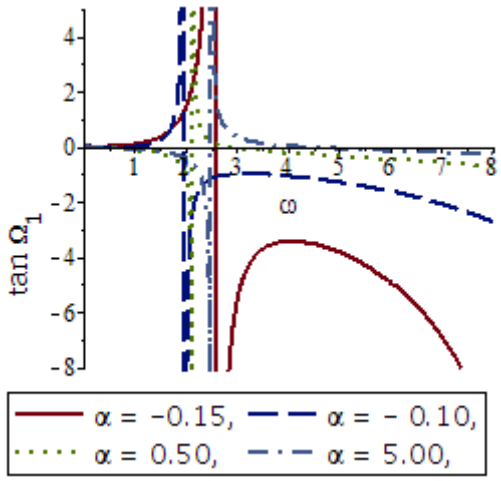

Fig.3. Phase of concentration profiles $(\tan\Omega_1)$

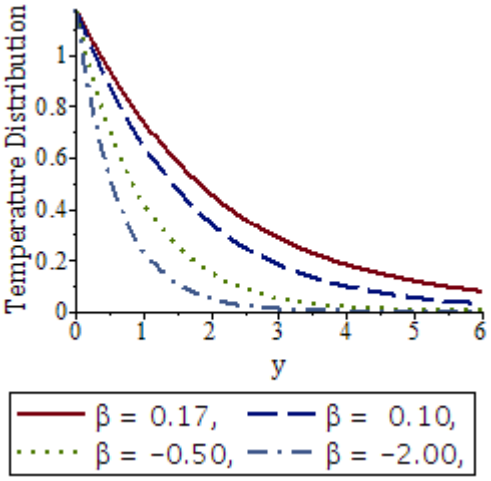

Fig.4. Transient temperature profiles β.

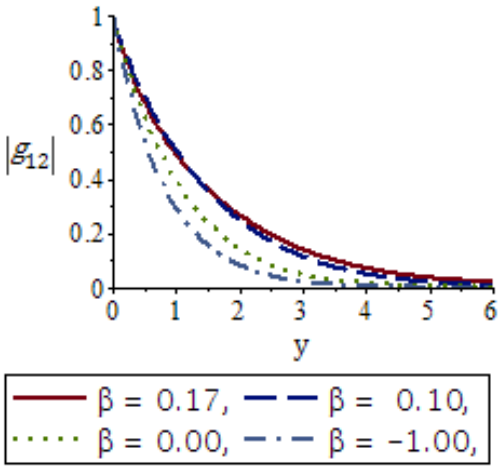

Fig.5. Amplitude of temperature profiles $(|g_{12}|)$.

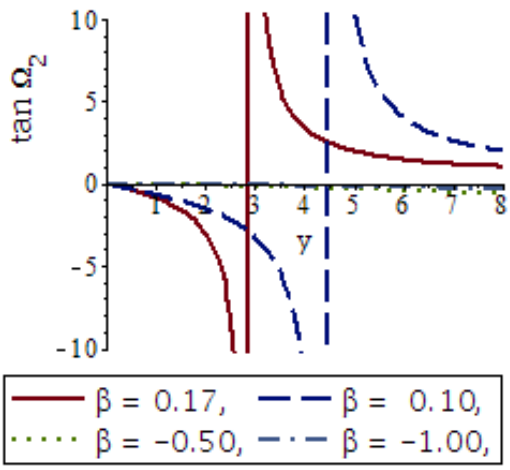

Fig.6. Phase of temperature profiles $(\tan\Omega_1)$.

to the surrounding reduces. Figure 6 illustrates the effect of the reaction parameter on phase concentration. The phase temperature is enhanced as heat is generated within the system. It is worth mentioning that heat absorption reduces the fluid temperature inside the flow boundary layer. This is because diffusion of heat from the fluid dynamics to the ambient produced lower bulk temperature.

4.3. Velocity field

The flow rate distribution is considered to varyless or more with the variations in the flow dependence terms. It should be mentioned here that the buoyance ratio $N > 1$ implies that the thermal buoyance dominates while $0 < N < 1$ implies that the mass buoyance dominates, and that N *positive* and N *negative* denote plate cooling and plate heating, respectively. The curves of Fig.7 show that an increase in the limiting surface velocity enhances the flow momentum profile. It is also observed that arise in the surface limiting velocity also increases the velocity boundary layer. The momentum fields against the position y for various values of heat generation/absorption (β) are displayed in Fig.8. The curves show that rising in the

generation heat $(\beta < 0)$ encourages the flow rate profile, while an increase in the heat absorption $(\beta > 0)$ brings about a decrease in the flow momentum field. One interesting inference of this finding is that maximum velocity is the surface velocity. The effects of the Grashof number (Gr) on the fluid flow are shown in Fig.9. The curves show that the mass buoyance number accelerates the fluid flow. Looking at the plot in Fig.9 more critically, it is seen that the difference in the flow velocity is highly significant with increasing mass buoyance force for the heated plate. For heating plate, maximum momentum profile close to the plate is observed for the rising values of Gr. In Fig.10, the flow velocity decreases as the term M increases. It is due to the effect of drag force (Lorentz force) that resists free movement of the fluid particles which in turn decreases the momentum distribution. The highest velocity is attained when this resistive type of force is zero, that is $M = 0$.

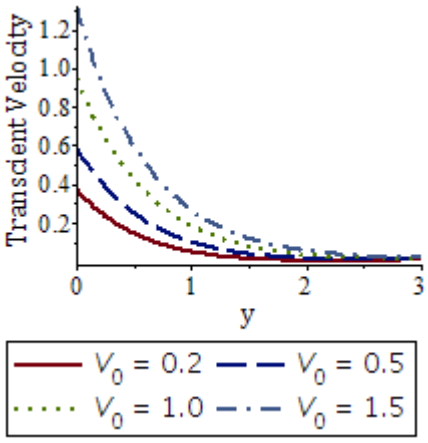

Fig.7. Transient velocity profiles for various values of V_0.

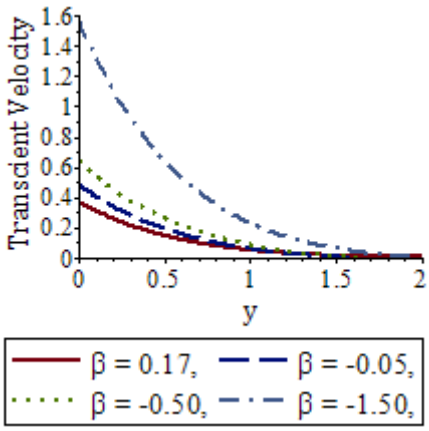

Fig.8. Transient velocity profile for various values of β.

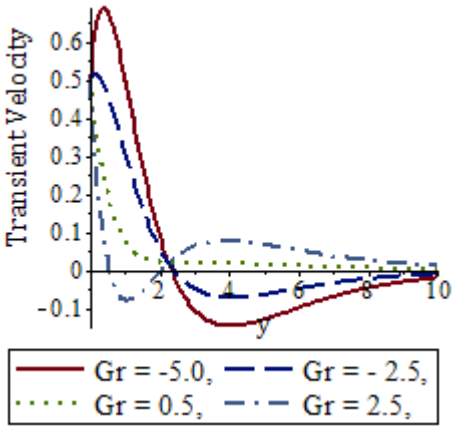

Fig.9. Transient velocity profiles for various values of Gr .

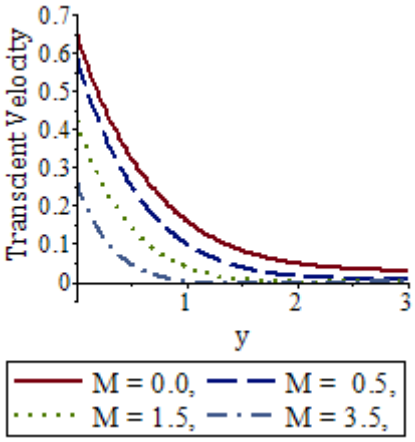

Fig.10. Transient velocity profiles for various values of M.

4.4. Rate of mass transfer, heat flux and skin friction

The wall mass transfer rate, temperature flux and fluid wall friction respectively described as the Sherwood number (Sh), skin friction (c_f) and Nusselt number (Nu) are displayed in Figs 11-16 for some

parameter values. Figures 11 and 12show the impact of the reaction term on the amplitude $|Sh_{12}|$ and mass gradient Shat the surface, respectively. The figures show that an increase in a generative reaction diminishes both the amplitude and mass gradient at the plate surface, while a destructive chemical reaction brings about an increase in the amplitude and concentration gradient at the surface. The amplitude of the transient heat gradient is seen to rise with a rise in the heat source term, either during heat generation or absorption process as depicted in Fig.13. The phase of temperature flux at the surface diminishes with a rise in both heat generation and absorption. Further, the phase of energy transport at the wall decreases as oscillating frequency increases for heat absorption as shown in Fig.14, while it increases with oscillating frequency for heat generation till it reaches a steady state. The skin friction is plotted against free stream oscillation for some selected flow parameters in Figs 15 and 16. It follows from Fig.15 that a rise in the value of *M* reduces the skin friction. Also, the skin friction is lower for a generative chemical reaction and higher for heat generation when compared with heat absorption case as shown in Fig.16.

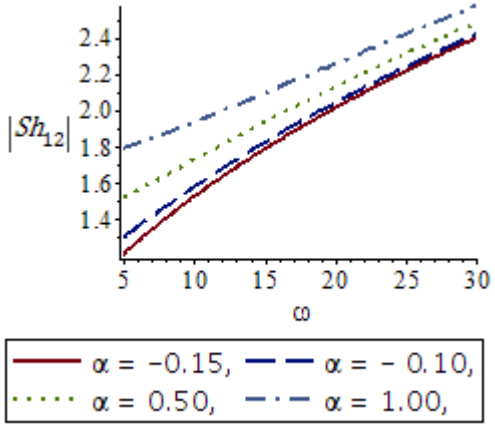

Fig.11. Amplitude of Sherwood number profiles $(|Sh_{12}|)$ for various values of α.

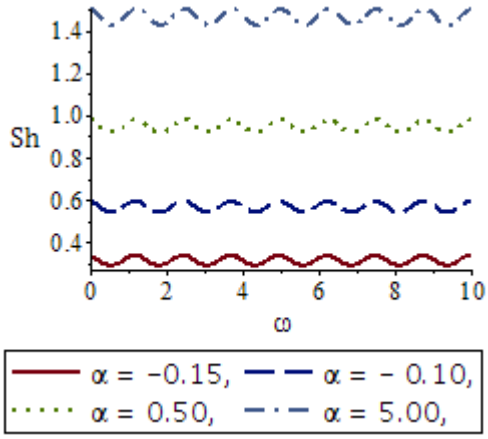

Fig.12. Transient Sherwood number profiles (Sh) for various values of α.

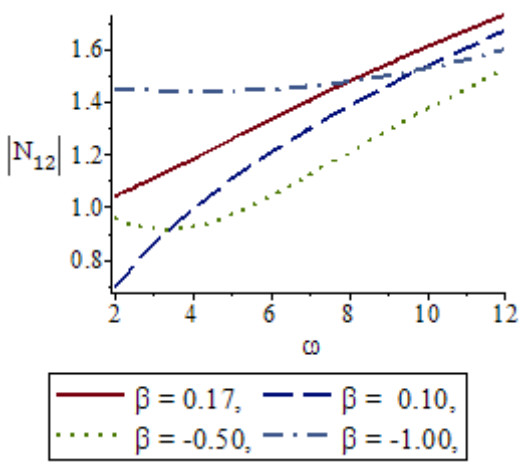

Fig.13. Amplitude of Nusselt number profiles $(|\mathrm{Nu}_{12}|)$ for various values of α $(\tan\Omega_5)$.

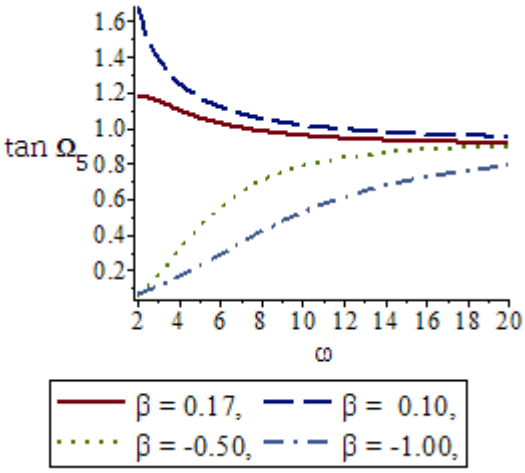

Fig.14. Phase of Nusselt number profiles for various values of β.

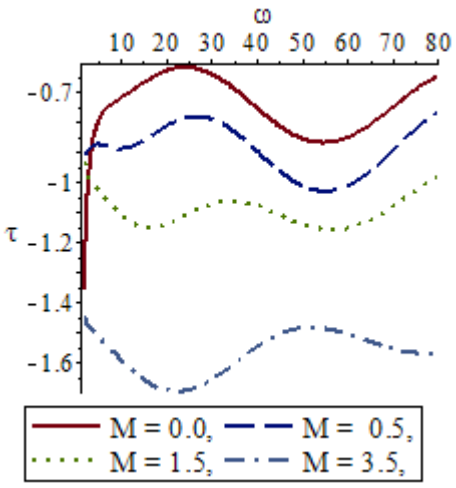

Fig.15. Transient skin-friction profiles τ for various values of M .

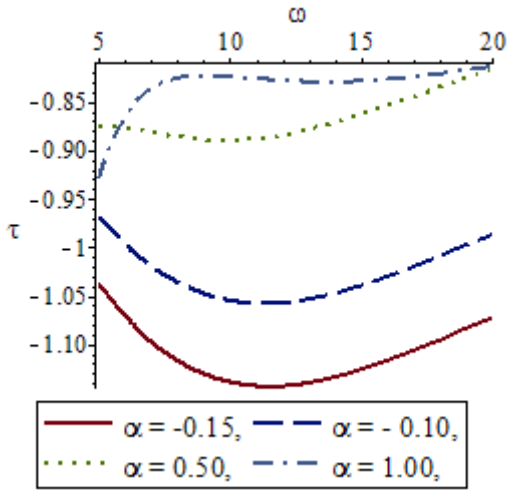

Fig.16. Transient skin-friction profiles τ for various values of α .

Conclusions

The transient flow of heat and mass transfer over an infinitely moved vertical permeable flat surface with chemical reaction, heat absorption/source and suction in a porous medium has been formulated and solved analytically by asymptotic expansions. The study revealed the subsequent physical interpretation and conclusions on the flow momentum, energy and mass distributions:

- flow concentration enhances with a rise in the chemical generative reaction and diminishes for the destructive chemical reaction.
- an increase in the heat absorption increases the temperature field while an increase in the heat generation enhances the temperature field.
- a rise in the heat generation increases the velocity of the flow field, while an increase in the heat absorption brings about a decrease in the velocity of the flow field.
- the phase of heat transfer at the wall diminishes with an increase in both heat generation and absorption.
- an increase in the buoyance ratio is observed to increase the velocity boundary layer.
- enhancing the reaction parameter brings about an increase in the mass transfer rate at the wall.

The flow reaction needs to be adequately controlled and monitored to avoid system blow up. As a result of some heat generation terms, the chemical reaction rate should be guarded.

Nomenclature

A – coefficient of permeability
C – concentration of the fluid
C_∞ – free stream species
D – species diffusivity
Gr – heat Grashof
g – gravity
k – heat conductivity
k_p – porosity
M – magnetic field
– mass Grashof
Pr – Prandtl number
Sc – Schmidt number
T – fluid temperature

T_∞ − free temperature
α − chemical reaction
β − heat sink/source
β_c − expansion mass volumetric
β_τ − expansion heat volumetric
ρ − fluid density
υ − fluid viscosity

References

[1] Salawu S.O. and Fatunmbe E.O. (2017): *Inherent irreversibility of hydromagnetic third-grade reactive Poiseuille flow of a variable viscosity in porous media with convective cooling*. − Journal of the Serbian Society for Computational Mechanics, vol.11, pp.46-58.

[2] Salawu S.O., Adebimpe O. and Olarewanju A.M. (2018): *Analysis of radiative heat absorption viscoelastic exothermic chemical reactive fluid with temperature dependent viscosity under bimolecular kinetic*. − Transylvanian Review, vol.35, No.32, pp.8339-8346.

[3] Noghrehabadi A., Ghalambaz M., Izadpanahi E. and Pourrajab R. (2014): *Effect of magnetic field on the boundary layer flow, heat, and mass transfer of nanofluids over a stretching cylinder.* − Journal of Heat and Mass Transfer Research, vol.1, pp.9-16.

[4] Das S., Jana R.N. and Chamkha A. (2015): *Unsteady free convection flow between two vertical plates with variable temperature and mass diffusion.* − Journal of Heat and Mass Transfer Research, vol.2, pp.49-58.

[5] Kareem R.A., Salawu S.O, and Yubin Yan (2020): *Analysis of transient Rivlin-Ericksen fluid and irreversibility of exothermic reactive hydromagnetic variable viscosity.* − J. Appl. Computes. Mech., vol.6, No.1, pp.26-36.

[6] Salawu S.O., Dada M.S. and Fenuga O.J. (2019): *Thermal explosion and irreversibility of hydromagnetic reactive couple stress fluid with viscous dissipation and Havier slips.* − Theoretical and Applied Mechanics Letters, vol.9, pp.246-253.

[7] Ogunseye H.A., Salawu S.O., Tijani Y.O., Riliwan M. and Sibanda P. (2019): *Dynamical analysis of hydromagnetic Brownian and thermophoresis effects of squeezing Eyring–Powell nanofluid flow with variable thermal conductivity and chemical reaction.* − Multidiscipline Modeling in Materials and Structures, vol.15, No.6, pp.1100-1120.

[8] Salawu S.O., Oladejo N.K. and Dada M.S. (2019): *Analysis of unsteady viscous dissipative Poiseuille fluid flow of two-step exothermic chemical reaction through a porous channel with convective cooling*. − Ain Sham Journal of Engineering, vol.10, pp.565-572.

[9] Salawu S.O., Hassan A.R., Abolarinwa A. and Oladejo N.K. (2019): *Thermal stability and entropy generation of unsteady reactive hydromagnetic Powell-Eyring fluid with variable electrical and thermal conductivities*. − Alexandria Engineering Journal, vol.58, pp.519-529.

[10] Stokes G.G. (1851): *On the effect of the internal friction of fluid on the motion of pendulum.* − Transactions Cambridge Philosophical Society, vol.9, pp.8-106.

[11] Turbatu S., Bühler K and Zierep J. (1998): *New solutions of the II Stokes problem for an oscillating flat plate.* − Acta Mechanica, vol.129, pp.25-30.

[12] Soundalgekar V.M., Pohanerkar S.G., Lahurikar R.M. and Birajdar N.S. (1995): *Mass transfer effects on flow past a vertical oscillating plate with variable temperature*. − Heat and Mass Transfer, vol.30, No.5, pp.309-312.

[13] Okedoye A.M. and Ayeni R.O. (2007): *Numerical solution of heat and mass transfer in MHD flow in the presence of chemical reaction and arrhenius heat generation of a stretched vertical permeable membrane.* − J. Nig. Ass. Math. Phy, vol.17, pp.111-118.

[14] Das S.S., Shaoo S.K. and Dash G.C. (2006). *Numerical Solution of Mass transfer effects on unsteady flow past an accelerated vertical porous plate with suction*. − Bull. Malays. Math. Sci. Soc., vol.29, pp.33-42.

[15] Das S.S., Satapathy A., Das J.K and Panda J.P. (2009): *Mass transfer effects on MHD flow and heat transfer past a vertical porous plate through a porous medium under oscillatory suction and heat source.* − Int. J. of Heat and Mass Transfer, vol.52, pp.5962-5969.

[16] Salawu S.O. and Dada M.S. (2018): *Lie Group Analysis of Soret and Dufour effects on radiative inclined magnetic pressure-driven flow past a Darcy-Forchheimer medium.* − Journal of the Serbian Society for Computational Mechanics, vo.12, pp.108-125.

[17] Soundalgekar V.M., Das U.N. and Deka R.K. (1997): *Free convection effects on MHD flow past an infinite vertical oscillating plate with constant heat flux.*− Indian Journal of Mathematics, vol.39, No.3, pp.195-202.

[18] Revankar S.T. (2000): *Free convection effect on flow past an impulsively started or oscillating infinite vertical plate.*− Mechanics Research Comm., vol.27, pp.241-246.

[19] Keimanesh R. and Aghanajafi C. (2016): *Analysis of radiation heat transfer of a micropolar fluid with variable properties over a stretching sheet in the presence of magnetic field*.− Journal of Heat and Mass Transfer Research, vol.1, pp.9-19.

[20] Rajput U.S. and Kumar S. (2011): *MHD flow past an impulsively started vertical plate with variable temperature and mass diffusion.*− Applied Mathematical Sciences, vol.53, pp.149-157.

[21] Moniem A.A. and Hassani W.S. (2013): *Solution of MHD flow past a vertical porous plate through a porous medium under oscillatory suction.*− Applied Mathematics,vol.4, pp.694-702.

[22] Ahmed N., Goswami J.K. and Barua D.P. (2013): *Effect of chemical reaction on an unsteady MHD flow past an accelerated infinite vertical pate with variable temperature and mass transfer.*− Indian journal of Pure and Applied Mathematics, vol.44, No.4, pp.443-466.

[23] Chen H., Zi Meng, Feng J. and Qingyun He (2014): *Effect of electromagnetic coupling on MHD flow in the manifold of fusion liquid metal blanket.*− Fusion Engineering and Design, vol.89, pp.29-35.

[24] Pattnaik J.R., Dash G.C. and Singh S. (2015): *Radiation and mass transfer effect on MHD flow through porous medium past an exponentially accelerated inclined plate with variable temperature.*− Ain Shams Engineering Journal, vol.8, pp.67-75.

[25] Abdelraheem A. (2019): *Radiation and chemical reaction effects on unsteady coupled heat and mass transfer by free convection from a vertical plate embedded in porous media.*–Journal of Heat and Mass Transfer Research, 10.22075/jhmtr.2019.10763.1149.

[26] Hemamalin P.T. and Kumar N.S. (2015): *An unsteady flow past an accelerated infinite vertical plate with the variable temperature and uniform diffusion through the porous medium.*− IOSR Journal of Mathematics, vol.11, No.3, pp.78-85.

[27] Salawu S.O., Ogunseye H.A. and Olanrewaju A.M. (2018): *Dynamical analysis of unsteady Poiseuille flow of two-step exothermic non-Newtonian chemical reactive fluid with variable viscosity.* − Int. J. of Mechanical Eng. and Techno. vol.9, No.12, pp.596-605.

[28] Ashish P. (2017): *Transient free convective MHD flow past an exponentially accelerated vertical porous plate with variable temperature through a porous medium.*− Hindawi International Journal of Engineering Mathematics, vol.23, pp.1-9.

[29] Okedoye A.M. and Salawu S.O. (2019): *Unsteady oscillatory MHD boundary layer flow past a moving plate with mass transfer and binary chemical reaction.*− SN Applied Sciences, vol.9, pp.1586.

[30] Salawu S.O. and Ogunseye H.A. (2020): *Entropy generation of a radiative hydromagnetic Powell-Eyring chemical reaction nanofluid with variable conductivity and electric field loading.* − Results in Engineering, vol.5, pp.100072.

[31] Okedoye A.M. and Salawu S.O. (2019): *Effect of nonlinear radiative heat and mass transfer on MHD flow over a stretching surface with variable conductivity and viscosity.*− Journal of the Serbian Society for Computational Mechanics, vol.13, No.2, pp.87-104.

Received: December 23, 2019

Revised: April 27, 2020